NASA TM-87123

NASA Technical Memorandum 87123
AIAA-85-2017



# An Experimental Study of Energy Loss Mechanisms and Efficiency Considerations in the Low Power dc Arcjet

Francis M. Curran
*Lewis Research Center*
*Cleveland, Ohio*



Prepared for the
Eighteenth International Electric Propulsion Conference
cosponsored by the AIAA, JSASS, and DGLR
Alexandria, Virginia, September 30-October 2, 1985



NASA

AN EXPERIMENTAL STUDY OF ENERGY LOSS MECHANISMS AND EFFICIENCY CONSIDERATIONS IN THE LOW POWER dc ARCJET

Francis M. Curran
National Aeronautics and Space Administration
Lewis Research Center
Cleveland, Ohio 44135

## Abstract

The potential utility of the low power dc arcjet in the field of auxiliary propulsion has motivated research activities at NASA Lewis Research Center and elsewhere. Early work in the field indicated that improvements in the areas of stability, energy efficiency, reliability, and electrode erosion would be necessary to obtain a useful device. Experiments with a water-cooled arcjet simulator were performed to investigate both the energy loss mechanisms at the electrodes and the stability of different conventional arcjet configurations in the presence of a vortex flow field. Although a full parametric study has not been completed, preliminary results show that in certain configurations only 25 to 30 percent of the input energy is lost to the electrodes. Results also show that vortex stabilization is not difficult to obtain in many cases at the flowrates used (0.054 to 0.096 g/sec $N_2$) and that a careful starting procedure is effective in minimizing electrode damage.

## Nomenclature

| | |
|---|---|
| A | anode area, $cm^2$ |
| D | constrictor diameter |
| E | distance anode tip extends down constrictor at start of test (Note: negative values indicate anode tip was on the upstream side of the constrictor entrance plane at start) |
| e | electron charge |
| G | electrode gap setting |
| $h_a$ | enthalpy in gas layer near anode surface |
| $h_{ps}$ | enthalpy in plasma stream |
| I | current, amps |
| k | Boltzmanns constant |
| $k_1$ | heat transfer coefficient |
| L | constrictor length |
| $P_A$ | power collected at anode, W |
| $P_{cold}$ | measured line pressure with no power input to arc |
| $P_{hot}$ | measured line pressure with arc running |
| $P_{IN}$ | arc total input power, W |
| $Q_R$ | heat radiated from column to anode, W |
| $Q_{TAL}$ | heat input to anode, W |
| $T_e$ | electron temperature, K |
| $U_{AF}$ | anode fall voltage, V |
| V | arc voltage, V |
| $V_{CONV}$ | convective energy term expressed as a voltage |
| x | exponent in Eq. (2) |
| $\alpha$ | half angle of diverging section of the anode nozzle |
| $\beta$ | half angle of converging section of the anode nozzle |
| $\phi$ | material work function, V |

## Introduction

Arcjets were first considered for space propulsion in the mid-1950's. Research and development of the concept was continued until the middle of the next decade. The results of the various programs were reviewed by Wallner et al., in 1965.[1] During this period major emphasis was placed on primary propulsion and most of the development centered at the 30 kW power level[2-5] assuming space power would be provided by nuclear electric systems.[6] Typically, hydrogen was used as the propellant to obtain specific impulse values in the 900 to 1500 sec range with efficiencies near or above 40 percent. Among the more notable accomplishments were a 30 day continuous life test at a specific impulse greater than 900 sec with 40 percent efficiency,[2,3] and a 500 hr life test of a regeneratively cooled thruster with a 54 percent peak efficiency.[4,5] Ammonia was also run successfully at this power level[3] although tests longer than 50 hr in duration were not performed. Research at the power levels available to near term electric propulsion (0.5 to 1.5 kW) was much less extensive. Low power arcjet technology efforts were undertaken by the Plasmadyne Corporation under contract to NASA.[7] This effort produced a radiation-cooled hydrogen engine that was life tested for 150 hr. During the test the efficiency level was near 30 percent and the specific impulse averaged approximately 920 sec. This test was voluntarily terminated and inspection showed little electrode wear. It was concluded that further optimization of the engine was possible but this was not pursued and low power arcjet technology programs in the USA were discontinued by 1965.

Currently the arcjet is being reexamined for applications to satellite propulsion at Lewis Research Center.[8,9] This is mainly because specific impulses on the order of 400 sec are

thought to be available with storable propellants. Since the best available technology gives a maximum specific impulse of about 320 sec this performance improvement would yield a propellant mass savings of at least 20 percent for a given total impulse requirement.

One of the major goals of the experiments described herein was to find the factors involved in obtaining stable operation of the conventional arcjet thruster design. Energy transfer processes near the electrodes were also studied for their effects on efficiency, lifetime, and reliability. To these ends a modular, water-cooled arcjet simulator was constructed in which cathode and anode pieces could be quickly replaced to facilitate parametric experiments. The arc chamber was built with gas passages that produced a vortex pattern of variable strength. Although the full parametric study is not complete, the initial results reported here point to a number of interesting positive conclusions about stability, energy transfer, and electrode erosion.

## Apparatus

### Flow System

A schematic diagram of the arcjet experimental arrangement is given in Fig. 1. The chamber containing the arcjet simulator was a Pyrex cross which was attached to a gate valve on a test port of a 1.83 m diameter by 5.49 m long pumping facility. The pumping capacity of the facility has been described elsewhere.[8] In typical experiments nitrogen was used as the working fluid and the flow rate ranged between 0.054 and 0.094 g/sec (2600 to 4700 SCCM). With no power input to the simulator the background pressure for these flow rates was less than 5 Pa (40 mtorr) while at peak power levels the background pressure increased to near 10 Pa (75 mtorr). The background pressure was monitored with a thermocouple gauge. The gas flow rates were monitored with transducers that relate thermal changes in a heated capillary tube to mass flow rates.

### Power

In most of the test a dc power supply with a maximum rating of 100 A at 110 V was used. For the ballast resistance shown in Fig. 1, paralleled sets of high current 0.5 and 1.0 $\Omega$ resistors were used. These could be easily added to or removed from the system, and it was found that a combination producing 1.5 $\Omega$ of resistance gave adequate stability. The voltage drop across this resistance occasionally limited the maximum current available in the highest power cases. The low total output capability of the power supply may have limited the minimum operable current level. In later tests a 150 V supply with a maximum current rating of 70 A was used, with a transistorized voltage regulator, to run the arc. A 1000 V low current power supply was used to start the arc. This supply was placed in parallel with the main supply, as shown in Fig. 1, and fitted with a high voltage diode to protect the main power supply. Arc current was monitored with a 50 mV to 50 A shunt, and the arc current and arc voltage measurements were fed through isolation amplifiers to a microprocessor controlled data recorder.

### Thrustor Simulator

Electrodes. To perform the parametric studies described herein, a modular arcjet simulator was used. Anodes and cathodes could quickly be replaced. A general schematic is shown in Fig. 2(a) and a photograph of one particular simulator is shown in Fig. 2(b). The anode and cathode inserts were held in brass electrode holders made to thread into their respective copper cooling jackets. The cathodes used were 0.32 cm diameter 2 percent thoriated tungsten rod stock ground to a 30° half angle tip. In a typical experiment the tip would extend approximately 2.22 cm from the brass holder. The anode inserts were machined from 0.64 cm diameter thoriated tungsten rod stock. The final design used in the 150 hr life test performed by the Plasmadyne Corporation incorporated a 30° half angle on both the nozzle and arc chamber sides of the constrictor.[7] These dimensions were used in all experiments described herein to form a basis for comparison for future work. The constrictor length and diameter, shown in Fig. 3, were varied from test to test as shown in Table I. The machined anode pieces were press fit into brass holders as shown in Fig. 2. This procedure was found to provide electrical contact and an effective gas seal. The cathode and anode were isolated from ground to prevent arcing from the nozzle to the vacuum tank.

Insulator/inlet. To isolate the anode and cathode, complete the arc chamber, and provide the gas passages a boron nitride piece was machined to fit into the 2.54 cm copper sleeve that extended from the anode cooling jacket. The chamber was 0.64 cm in diameter, to match the anode insert, and its depth was 0.32 cm. A step was machined on the face of the insulator to accommodate a gasket which prevented gas leakage. This is shown in Fig. 2. Circular slots were machined on the outside of the insulator to carry the gas flow to tangential and axial inlet holes, 1.07 mm in diameter. The holes were sealed from each other and from the chamber by O rings. Gas leaks around the cathode water jacket were also eliminated by an O ring. The swirl pattern was obtained by positioning the tangential gas inlets as shown in Fig. 4. Axial inlets were also drilled, as shown, so that some axial velocity could be imparted to the flow. Arc chamber pressure was normally monitored in both lines. The two readings were considerably different in the experiments. The axial holes faced directly into the chamber and were not on walls in direct contact with the swirling gas pattern. In the typical experiment the axial flow was not used and the inlet ports were used only as pressure taps.

Cooling system. The inlet and outlet connections to the cooling water jackets were fitted with thermocouples to monitor temperatures of water circulated through the electrode assemblies as were the connections to the gas cooling jacket installed to protect the Pyrex cross and gate valve (Fig. 1). Deionized cooling water flow was provided by commercial water bath units, and water flow rates were calibrated by using a stopwatch and known volumes. Chromel-constantan thermocouples were used in the anode and gas cooler water lines. Thermocouple readings were logged on the automatic chart recorder and were also checked frequently against readings taken with a

mercury thermometer immersed in the flow stream. Although the cathode and anode thermocouples were ungrounded and deionized water was used for cooling, a small amount of current did flow in the cathode water lines. At the highest current settings this leakage was measured at approximately 25 mA and caused problems in cathode cooling water temperature measurements. to circumvent this, the cathode thermocouples were monitored by a separate unit, equipped to allow 0.1 °C resolution, isolated from ground through an isolation transformer. For this, iron-constantan thermocouples were used and readings were logged by hand.

Plume rake. To obtain a rough estimate of plume stability and extent a thermocouple rake was positioned approximately 10 cm downstream from the nozzle exit plane. Five platinum-platinum/rhodium thermocouples were used in these initial experiments, spaced 1.9 cm apart. The sheaths of the thermocouples were fitted with stainless steel aspirator tips. The central thermocouple was positioned slightly off the center line of the constrictor to avoid the highest temperature region but even so, its stainless steel aspirator tip did melt.

## Procedure

### Arc Starting and Changeover

Except in the first test performed for this study (test number 76) argon gas was always used to start the arc with the flow rate set at approximately 0.1 g/sec though the tangential inlet passages. In the first test various starting procedures were evaluated. The current level of the main power supply was set to the desired starting level, typically 25 A. The ignitor supply was then turned on and the voltage increased slowly until ignition occurred. The ignitor supply was left at the starting voltage until the arc plume was stable and then turned off. The thruster was operated on argon for an initial warm up period, usually from 5 to 10 min, and then the argon feed valve was closed and the nitrogen feed valve opened.

High purity argon (99.999 percent) was used to start the arc and high purity nitrogen (99.998 percent) was used in all tests. Photographs of the apparatus running with argon and nitrogen are shown in Figs. 5(a) and (b), respectively. Most of the argon excitation is bounded by a 60° included angle plume.

### Burn-in Period

Upon analysis of initial test data it became apparent that the performance varied considerably during an initial "burn-in" period the first time the thruster was operated with new electrodes. Usually, after this period a steady state was reached in which the data were reasonably reproducible. Each new configuration was usually operated for 30 min to 1 hr, with nitrogen gas at about 0.05 g/sec and 25 A, before any data were taken. The cause for this burn-in period will be discussed in the following section.

### Parametric Variation and Data Collection

For each anode insert a new cathode was used and set for the desired gap width, defined as shown in Fig. 3. The arc chamber pressure was then measured, with no power input, at the flow rates to be used in the tests. After the arc was started, and the burn-in period completed, an initial set of data was taken. The initial data set was obtained with a flow rate of 0.075 g/sec. The current was set at various levels up to 35 A with the usual pattern being 25-20-30-35-15-25 A. The 25 A point was generally taken twice, before and after the others, to indicate whether or not significant operating changes had occurred. In later tests data at lower current levels were collected when possible. The procedure described above was repeated at flow rates of 0.054 and 0.096 g/sec. In some experiments data were also taken with the flow split between the axial and tangential passages. The splitting patterns used were 0.011 g/sec axial - 0.064 g/sec tangential and 0.023 g/sec axial - 0.052 g/sec tangential. Finally, the 25 A, 0.075 g/sec tangential flow data were normally repeated. A 5 to 15 min equilibration period was allowed between each change in current setting so a typical test configuration logged 5 to 6 hr of total operating time including 5 to 10 startups and shutdowns. The cathode was weighed before and after each test and in later tests the length was also measured before and after the test.

### Surface Analysis

Scanning Auger electron spectroscopy was used to analyze the surfaces of the electrodes used in test number 83. The tip, the conical shoulder, and a discolored portion of the barrel of the cathode were studied and compared to results obtained with an unused cathode. A coating on the nozzle side of the brass anode holder was also analyzed.

## Results and Discussion

The major objectives of these preliminary experiments were to obtain stability of operation and to observe trends over a wide range of cathode/anode (nozzle) configurations. Use of the vortex flowfield greatly increased overall stability. It should be noted that although some of the configurations detailed in Table I operated in a stable fashion over a wider range than others, a range of stable operation was found in every case.

### Power Input Characteristics

At present the power available for auxiliary propulsion applications ranges from 0.5 to 1.0 kW and growth to the 3kW level is possible.[10] In performing the tests, therefore, a range of currents was tried in order to examine the V-I characteristics and stability of each configuration. In almost every case studied the V-I curve generated showed only small changes in voltage with change in current for current levels 15 A and above. It was also found that few of the configurations would operate at currents less than 15 A. A typical data set showing V-I characteristics is shown in Fig. 6(a). In all tests the operating voltage was seen to increase with increasing flow rate. This result was expected. For a constant geometry, pressure increases with increasing mass flow rate. This increases the collision rates and so the rate at which energy is removed from the conducting column. Thus for

arc maintenance a higher voltage gradient is required. The highest voltage levels were obtained at the lowest current levels followed by a voltage minimum and then a gentle increase in voltage with current. This indicates that in the current range studied the voltage is relatively independent of current and so the power input to the simulator was linearly dependent on the current. This is shown in Fig. 6(b), and implies that simulator power level can be changed over a wide range with no shifts in operating mode.

The slopes of the plots obtained in each of the tests, at the three flow rates, are shown in Table II. Other data to be discussed later in this section show that the combined power losses at the anode and cathode rise more slowly than does the total power with current. This implies that as the total power increases the efficiency of energy input to the gas increases. From the table it can be seen that the 0.089 cm diameter constrictor with an L/D ratio of 1.14, i.e., test number 84, gave the highest values of input power to current ratio. The data from test number 78 show, however, that lowering the L/D ratio drastically (i.e., to 0.286), with the same constrictor diameter, did not cause a large change in the power to current ratio. The smallest diameter constrictor, used in test number 85, also produced high values of P/I as did the large diameter constrictor with the longest length, used in test number 76. Some anomolous behavior was observed at the lowest flow rate in this last test. The power input versus current plot displayed a large negative deviation from linearity at the high current end. This behavior points to a change in the fundamental operating mode of the arcjet simulator which will be discussed further.

The range of operation was dependent on the particular configuration but, in general, the arcs would not operate at current levels below 15 A. Typically, when the current level was lowered from 20 to 15 A the simulator would operate for some minutes and then go out before the end of the equilibration period. This is probably a thermal effect. As the power input to the gas is decreased the boundary layer adjacent to the water cooled wall will probably change. Lowering the current in this range implies a change in the width of the arc channel and the interaction between these two could lead to a breakdown in the flow pattern which could extinguish the arc. It is doubtful that this represents a fundamental limitations on power input especially in the case of the hot walled thruster. In one test the thruster ceased operation, as described above, at 20 A. A restart produced successful operation at 20 A.

A very notable exception to the above mentioned behavior was found in test number 85; here stable operation was demonstrated at current levels down to 3.8 A. In this test a short constrictor (0.025 cm) was used. Figure 7 shows the arc characteristics for the low current operation. Obviously, the voltage gradient increases rapidly in the low current mode and this causes a positive deviation from linearity in the arc power curves. Other data, to be discussed further, indicate that little of this power is input directly to the gas, however.

## Electrode Losses

The calorimetric data were taken both to illustrate the efficiency of a particular configuration for inputting energy into the propellant and to provide insight into the energy loss mechanisms involved at the electrodes. Both high and low power water cooled simulators were studied in the early 1960's.[11,12] In the former, a water-cooled, 0.5 lb hydrogen thrustor was found to lose about 54 percent of the input energy to the electrodes while its hotwalled counterpart lost only about 15 percent of the input radiatively.[11] Low power tests, using hydrogen and helium as propellants, were performed by the Plasmadyne Corporation.[12] In these, various nozzle configurations were run under a number of conditions. It was found that cooling losses could be reduced to 60 percent from the 80 percent level by doubling propellant flow and current. Losses decreased with increasing swirl strength from 75 to about 60 percent. By reducing the cooling to a point where the nozzle was white hot the losses dropped to 33 percent from nearly 60 percent. Finally, arc length was found to affect the power input characteristics but not the cooling loss. These results form some basis for comparison with those presented here.

Throughout the series of tests only a small amount of energy was found to be drawn from the cathode. Only small temperature differences were observed between the input and output streams of the cathode calorimeter (typically 1 to 2 °C). While these small temperature differences made precise quantification of the energy loss difficult, the obvious conclusion is that cathode energy losses were between 1 and 5 percent of the total power input and were not a major source of inefficiency. The energy deposited at the cathode also did not vary much with current or total input power. Typical results are illustrated in Fig. 8. This indicates that the percentage of power lost to the cathode actually decreases with increasing arc power input. The cathode was immersed in the cooling gas flow and was forced, by the gas flow, to emit from the tip which extended far from the cooling jacket. Because of this, low energy input to the cathode calorimeter was expected. Thermionic emission, as described by the Richardson-Schottkey equation, is an exponential function of temperature. After a certain current level is reached, then, only small increases in temperature accompany current increases. The data are consistent with this as small temperature changes produce only small changes in heat conduction to the calorimeter. In fact, examination of the cathode after each of the tests showed that the tip had been molten during operation. This implies that the operating temperature of the cathode tip remained fixed at the melting point of the cathode material so changes in conductive losses would be expected to be small.

Power losses at the anode were, as expected, much larger than those found at the cathode. This power dissipation showed a marked dependence on current as, in almost every case, the anode loss was directly proportional to the current level. The slopes of the anode power loss versus current plots for all the tests are given in Table III. Also included are the ratios of the total power lost at the lowest and highest current levels used in the least squares analysis of the data. A

typical data set is plotted in Fig. 9. A large body of data has been accumulated on anode loss mechanisms in arc experiments. A simplified equation often used to describe the heat transfer to the anode is given as:[13]

$$Q_{TAL} = Q_R + k_1A(h_{ps} - h_a) + I\left[\left(\frac{5kT_e}{2e}\right) + \phi + U_{AF}\right] \tag{1}$$

While the radiative term, first on right, is expected to be small and constant with current for a nitrogen arc at moderate pressure the second, or convective, term is not. This term is highly dependent on boundary layer effects and, as the total energy in the plasma is directly proportional to the current level, is expected to be some function of current. The first term under the parenthesis in Eq. (1) represents the kinetic energy brought with the electron to the anode surface not acquired in the anode fall. This thermal contribution to the anode loss is not large, probably well under 1 eV and is not expected to vary much with changes in flow rate. The second term under the parenthesis is solely dependent on the work function of the electrode material and so also should not vary with flow rate. The last term represents the energy gained by the election as it passes through the anode fall to the anode. The magnitude of the anode fall is related to the ease with which ions are formed near the anode. This voltage drop is expected to decrease with increasing plasma temperature.[14] It has been suggested that the anode fall is very small and that contraction of the anode attachment can be avoided in arrangements in which an ionized plasma is forced past a cooled anode surface, such as in the arcjet.[15] One of the major reasons for using the vortex flow field, in addition to its effect on stability, is to reduce the heat transfer rate to the walls of the anode/nozzle by keeping a dense relatively cool layer of gas circulating near the anode. This has been demonstrated in the past.[12] That this occurs here, can be seen by examining the data in Table III and the aforementioned terms from the parenthesis of Eq. (1). From the data it can be seen that in each case, save one, the anode losses are reduced with increasing flow rate. In the single exception the data did not correlate well and are considered anomolous at this point. Returning to Table II, it is seen that as the flow rate is increased from 0.054 to 0.096 g/sec (i.e., by a factor of nearly 1.8) the total power input to the arc increases by only 15 to 20 percent. Thus, the gas temperature near the anode should decrease with flow rate. This would imply an increasing anode fall, if a change were to occur, and so an increase in anode losses as the other terms under the parenthesis in Eq. (1) are approximately constant as discussed previously. This is opposite the observed trend. The convective term, therefore, is probably responsible for the decrease in anode heat loading and this term is a function of current. This means Eq. (1) can be modified as:

$$Q_{TAL} = Q_R + I[V_{CONV}]^x + I\left[\frac{5}{2}\frac{k}{e}T_e + \phi + U_{AF}\right] \tag{2}$$

in which x takes on a value of nearly one if the anode fall voltage is small and nearly constant as suggested. It should be noted that in the hot-walled design the convective term should act to increase the enthalpy of the gas near the anode surface and so increase the overall device efficiency.

Before leaving Table III one final observation should be made. Anomolous behavior was observed at the low flow rate setting in test number 76. In this test the heat transfer to the anode was higher than in any other current setting but at the highest current setting the power input versus current curve showed a large, negative deviation from linearity. Plume stability was also observed to be very poor. This test involved the anode insert with the largest dimensions used. The observations seem to indicate that, at the high current level, there was a breakdown in the vortex stabilization of the arc with the point of anode attachment then moving back down the constrictor wall. Other tests, not reported in detail here, support this conclusion. In these tests, the strength of the vortex was not sufficient to force the arc down the constrictor. No luminous plume was observed, the voltage (and total power) was quite low and almost all of the input energy was recovered at the electrodes - mostly at the anode.

In general, the percentage of the total power lost at the anode is between 20 and 25 percent of the total input power. Since the cathode losses are only 1 to 5 percent of the input power, the swirl stabilized simulator was normally around 70 percent efficient in depositing energy into the propellant. These figures are encouraging as the losses are smaller than those found in the 1960's studies described earlier.

## Electrode Condition and Burn-in

In early tests, before high argon flow rates were used in the starting procedure, the cathodes showed visible erosion away from the tip near the boron nitride insulator. This type of damage was eliminated when the full vortex flow field was used at startup. The vortex was found to force emission from cathode tip since the exposed cylindrical portions of the cathode pieces were smooth. Molten material was visible at the tip of every cathode and, in the cases where measurements were taken, the cathode length had decreased. Results of surface analysis of the tip region of the cathode used in test number 83 were similar to those from an unused cathode. From test to test the tips varied greatly in appearance. In some cases a large molten ball formed as shown in Fig. 10. This cathode tip was used in test 76 and was, by far, the most damaged of the lot. This particular cathode had been used in earlier tests in which the full vortex flow field was not used at startup and the shoulders show the familiar, sandblasted appearance that occurs before the transition from glow to arc discharge. In other tests the cathodes showed less mass loss. Some exhibited only a rounding at the tip and a slight polishing of the shoulders, e.g., Fig. 11; test number 80. In the tests with 0.035 and 0.025 inch diameter constrictors the cathode tip took on a raised appearance. The tips from tests 78 and 84

resembled cylinders that roughly conformed to the shape of the constrictors. Figure 12 shows the cathode used in test 78. As with all the cathodes started under high flow rates the cathodes shown in Figs. 11 and 12 show little of the sandblasted effect illustrated in Fig. 10. Less damage was caused under starting conditions where less time is spent in the glow discharge mode and so this type of damage is avoided. With the exception of the cathode from test 76 very little mass loss was observed. The cathode from data set 78 had the highest total loss at 6 mg. This cathode was run at various conditions for approximately 6 hr. The cathode from test 84 showed a weight loss of <1 mg. These data indicate that under proper conditions material evaporated from the molten cathode is apparently redeposited and redistributed on the cathode if the proper conditions are maintained.

As with the cathodes, the anodes generally showed little damage. The anode used in test number 84 is typical and shown in Fig. 13. There is no obvious erosion of the constrictor or in the diverging section of the nozzle. Surface analysis of the nozzle used in test 83 showed a thin coating of tungsten nitride in the diverging section of the nozzle. One of the unanswered questions about conventional arcjet operation is the mode of anode attachment. The condition of the nozzles seems to imply a diffuse attachment primarily in the diverging portion of the nozzle. The general homogenity of the plumes observed also points to this. Some wobbling in the plume and streamers which develop (Fig. 5(b)) weaken this conclusion. The anode from test 76, however, did show considerable damage with molten tungsten in the diverging section, Figs. 14(a) and (b). It is possible that damage occurred while the simulator was running in the aforementioned unstable mode. From the conditions of the cathodes before and after the tests it is apparent that the burn-in period, in which performance changes gradually with time under set conditions, is caused by changes in the cathode as it gradually takes on a steady state shape. The changes in performance are manifested in slight increases in operating voltage level and line pressure. Once the steady state is obtained predictable operation can be expected if erosion can be kept in check.

### Performance

Estimates of performance without an actual thrust measurement are questionable for a number of reasons. First, the chamber pressure must be accurately measured. As discussed in a previous section, the pressure measurements taken upstream in the two propellant lines did not match so an accurate measurement could not be assumed. The nozzle thrust coefficients were also unknown. The only definite indication that thrust was increasing with increasing input power (or current) was that both pressure measurements continued to increase with increasing power input, at a fixed flow rate, except at the very low current levels in test number 85. This is illustrated in Fig. 15. Shown is the line pressure ratio measured with propellant flowing to the thrustor simulator with and without power input. At the low current values the arc was seen to flicker and some melting was observed near the constrictor entrance on the converging side of the nozzle. This probably indicates that the arc attachment point had moved back down the constrictor throat.

Rough performance estimates indicated that the actual efficiency was quite low. This was expected as nitrogen is not an optimal propellant.

## Concluding Remarks

A number of conclusions can be drawn from the observations and preliminary data presented in this report. Certainly, imposition of the vortex flow field was effective in producing stable operation over a wide range of configurations and operating conditions with nitrogen propellant. The expected difficulties with arc stabilization at low current levels was observed.

A very carefully controlled starting procedure incorporating the swirling flow was found to force the arc to start from the cathode tip, thus reducing cathode damage. This indicates that careful attention to starting mechanism will be necessary for an integrated propulsion system.

Close examination of the thrustor behavior with time and of the condition of the cathode both before and after the tests have shed light on the so called "burn-in" period necessary before reliable, predictable operation of the thrustor is attained. Indications are that during the burn-in period, at least in the water cooled simulator, the cathode is reshaped to nearly a steady state condition, and so the conditions in the arc chamber, particularly near the cathode, are changing throughout the period. This is probably responsible for performance changes during the period. From general observations it is suggested that extreme care be taken in thrustor manufacture and assembly to insure a symmetrical chamber. This and other precautions such as rounding of sharp edges and a careful starting procedure should increase both thrustor reliability and lifetime.

Energy balance measurements indicated less than 5 percent of the total arc power was lost to the cathode assembly. Losses at the anode were typically in the 20 to 25 percent range. Some configurations were more effective than others at inputting energy to the arc. The constrictor dimensions seemed to be more important in determining range of operation than power input. This was expected as the residence time in the constrictor is not long enough for any recombination to occur. It is clear that if a thrustor can be made to operate in the proper mode, with the arc pushed down the constrictor, only a relatively small percentage of the input power (approximately 25 percent) is lost to the electrodes even under water cooled conditions where convective heating of the propellant is lost. Smaller electrode losses are expected in hot-walled, radiation cooled designs which also use regenerators to heat propellants and cool electrodes. Even though a quantitative performance estimate was not made it was obvious that the efficiency of operation was low. Conventional arcjet designs are highly susceptible to frozen flow losses and flight application of the

arcjet thrustor will be keyed to operation in an optimum specific impulse range for the propellant of choice.

The water-cooled thrustor simulator has been shown to be a very versatile tool for the investigations of arc stability, energy transfer, and starting processes. Further tests with different propellants under both hot- and cooled-wall conditions are necessary to complete the design definition of an operational flight unit. Construction of facilities for these tests is now in progress.

## REFERENCES


1. Wallner, L.E. and Czika, Jr., J., "Arc-Jet Thrustor for Space Propulsion," NASA TN-D-2868, 1965.
2. John, R.R., Connors, J.F., and Bennett, S., "Thirty Day Endurance Test of a 30 kW Arc Jet Engine," AIAA Paper 63-274, June 1963.
3. John R.R., "Thirty Kilowatt Plasmajet Rocket-Engine Development," Avco Corp., Wilmington, MA, RAD-TR-64-6, July 1964, (NASA CR-54044)
4. Todd, J.P. and Sheets, R.E., "Development of a Regeneratively Cooled 30 kW Arcjet Engine," AIAA Journal, Vol. 3, No. 1, Jan. 1965, pp. 122-126.
5. Todd, J.P., "Thirty kW Arc-Jet Thrustor Research," Report no. FR 024-10338 (APL-TDR-64-58), Giannini Scientific Corp., Mar. 1964.
6. "Arc Jet Application Study," General Electric Co., Sept. 1961. (NASA CR-140076).
7. McCaughey, O.J., Geideman, Jr., W.A., and Muller, K., "Research and Advanced Development of a 2 kW Arc-Jet Thrustor," Plasmadyne Corp, Santa Ana, CA, GRC-1646, 1963. (NASA CR-54035)
8. Nakanishi, S., "Performance Evaluation of a 1 kW Arcjet Thruster," AIAA Paper 85-2033, Oct. 1985.
9. Hardy, T.L., and Nakanishi, S., "Cathode Degradation and Erosion in High Pressure Arc Discharges," International Electric Propulsion Conference, 17th, Japan Society for Aeronautical and Space Sciences, Tokyo, 1984, pp. 560-573.
10. Kuninaka, H., Ishii, M., Kuriki, K., "Low Power DC Arcjet," AIAA Paper 85-2030, Oct. 1985.
11. Cann, G.L., Ducati, A.C., Giannini, G.M., and Stoner, W.A., "The Arc Jet," Proceedings, Symposium on Advanced Propulsion Concepts, 2nd, Oct. 7-8, 1959, U.S. GPO, Washington, D.C., 1960.
12. Stoner, W.A., "Investigation of a Low-Thrust Plasma Propulsion Device," Plasmadyne Corp., Santa Ana, CA, 1FR-021-1806, Feb. 1961.
13. Shih, K.T., Pfender, E., Ibele, W.E., Eckert, E.R.G., "Experimental Anode Heat-Transfer Studies in a Coaxial Arc Configuration," AIAA Journal, Vol. 6, No. 8, Aug. 1968, pp. 1482-1487.
14. Finkelnberg, W. and Maecker, H., Electric Arcs and Thermal Plasmas, Handbuch der Physiks, vol. 22, Springer, 1956.
15. Buhler, R.D., "Electro-Thermal Propulsion," Advances in Space Propulsion, Part II-Space Propulsion Systems, Section 3, UCLA, Pasadena, CA, July 1962, p. 48. (Short Course X458.1)


TABLE I. - THRUSTOR SIMULATOR DIMENSIONS

| Test number | D | | L | | G | | A | |
|---|---|---|---|---|---|---|---|---|
| | cm | inch | cm | inch | cm | inch | cm | inch |
| 76-77 | 0.13 | 0.050 | 0.13 | 0.050 | 0.066 | 0.026 | 0.084 | 0.033 |
| 83 | .13 | .050 | .10 | .040 | .066 | .026 | .043 | .017 |
| 82 | .13 | .050 | .10 | .040 | .094 | .037 | .015 | .006 |
| 80-81 | .13 | .050 | .025 | .010 | .11 | .045 | -.005 | -.002 |
| 84 | .089 | .035 | .10 | .040 | .066 | .026 | .010 | .004 |
| 78-79 | .089 | .035 | .025 | .010 | .066 | .026 | .010 | .004 |
| 85 | .064 | .025 | .025 | .010 | .066 | .026 | -.010 | -.004 |

TABLE II. - SLOPES OF POWER INPUT VERSUS CURRENT

| Test number | L/D | G | | Slope, W/A flow rates, g/sec | | |
|---|---|---|---|---|---|---|
| | | cm | inch | 0.054 | 0.075 | 0.096 |
| 76 | 1.0 | 0.066 | 0.026 | 32.5 | 43.5 | 47.9 |
| 78 | 0.28 | .066 | .026 | 42.2 | 46.3 | 50.1 |
| 80 | .20 | .011 | .045 | 29.9 | 32.2 | 36.4 |
| 82 | .80 | .094 | .037 | 33.3 | ---- | 39.5 |
| 83 | .80 | .066 | .026 | 33.7 | 38.1 | 39.5 |
| 84 | 1.14 | .066 | .026 | 46.4 | 50.8 | 54.2 |
| 85 | .20 | .066 | .026 | 42.6 | 44.7 | 48.8 |

TABLE III. - POWER INPUT AT ANODE PLOT SLOPES

| Test number | L/D | G | | 0.054 | | | 0.075 | | | 0.096 | | |
|---|---|---|---|---|---|---|---|---|---|---|---|---|
| | | cm | inch | Slope, W/A | $P_A/P_{IN}$ σ $I_{MIN}$ | $P_A/P_{IN}$ σ $I_{MAX}$ | Slope, W/A | $P_A/P_{IN}$ σ $I_{MIN}$ | $P_A/P_{IN}$ σ $I_{MAX}$ | Slope, W/A | $P_A/P_{IN}$ σ $I_{MIN}$ | $P_A/P_{IN}$ σ $I_{MAX}$ |
| 76 | 1.0 | 0.066 | 0.026 | 14.4 | 0.37 | 0.31 | 10.5 | 0.24 | 0.24 | 9.1 | 0.21 | 0.20 |
| 78 | 0.28 | .066 | .026 | 7.2 | .31 | .23 | 8.2 | .20 | .22 | 8.1 | .18 | .21 |
| 80 | .20 | .11 | .045 | 9.5 | .24 | .28 | 8.3 | .21 | .24 | 7.6 | .21 | .21 |
| 82 | .80 | .094 | .037 | 11.0 | .22 | .28 | ---- | .28 | .23 | 7.6 | .20 | .20 |
| 83 | .80 | .066 | .026 | 10.7 | .24 | .28 | 9.4 | .22 | .23 | 7.6 | .22 | .20 |
| 84 | 1.14 | .066 | .026 | 10.9 | .21 | .22 | 9.4 | .18 | .18 | 7.9 | .18 | .17 |
| 85 | .20 | .066 | .026 | 11.3 | .20 | .25 | 9.9 | .19 | .21 | 8.6 | .18 | .18 |

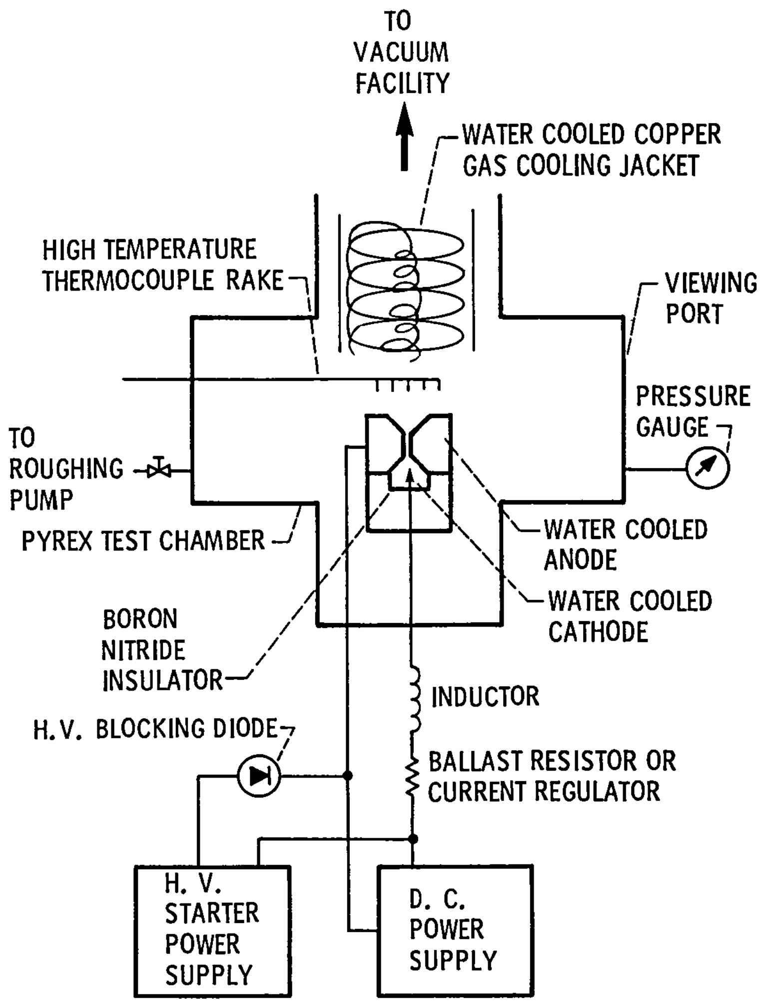


Figure 1. - Schematic diagram of experimental arrangement.

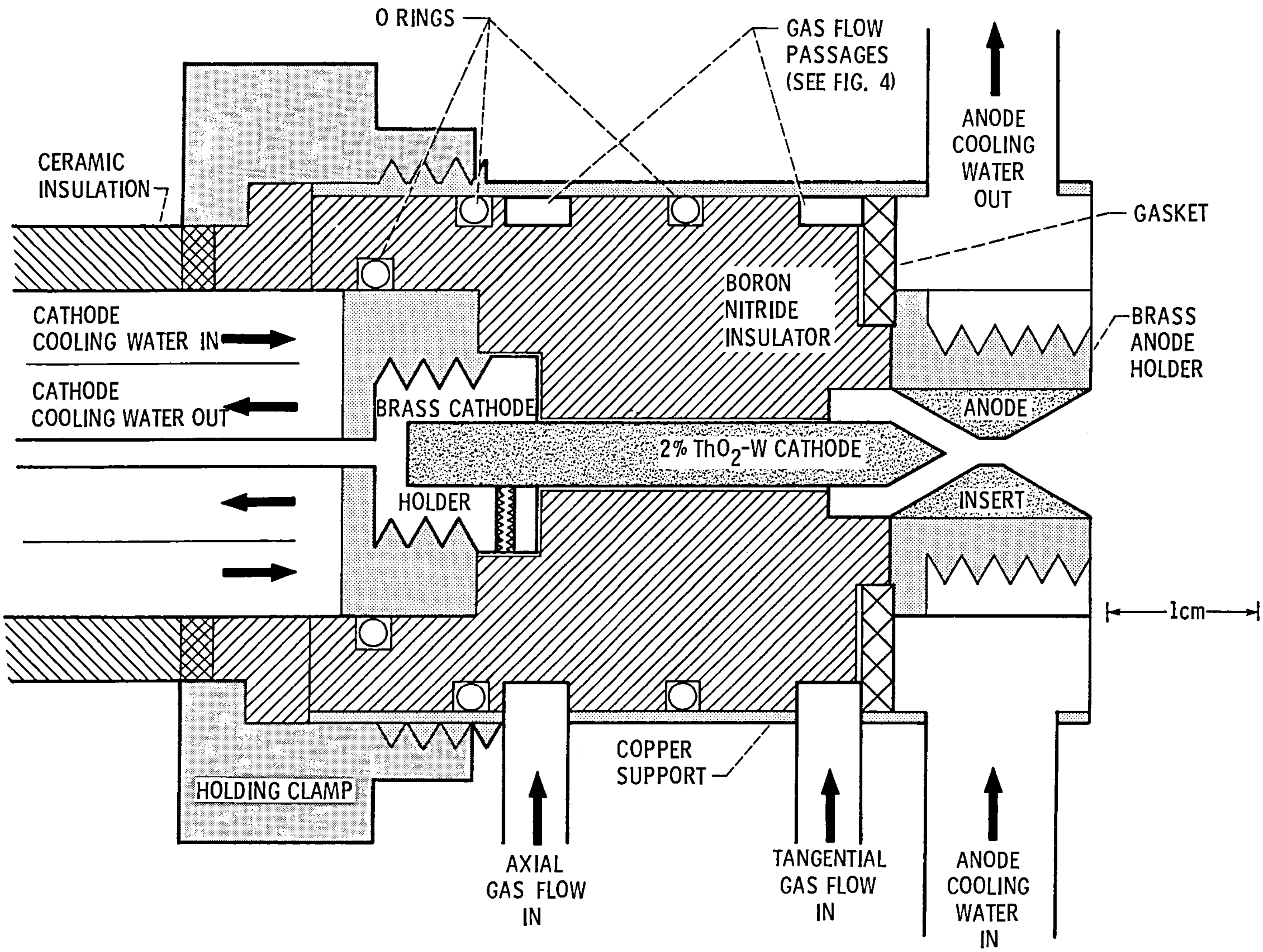


(a) Schematic diagram.

Figure 2. - Arc jet thruster simulator.

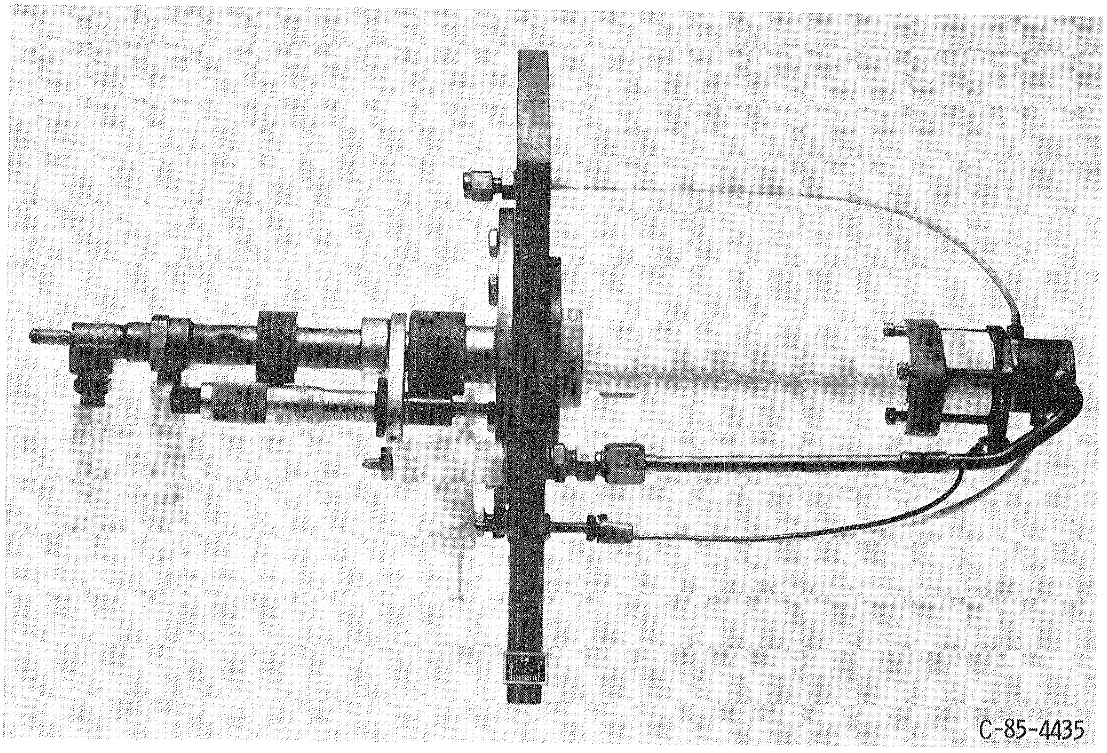


(b) Photograph of thruster simulator.

Figure 2. - Concluded.

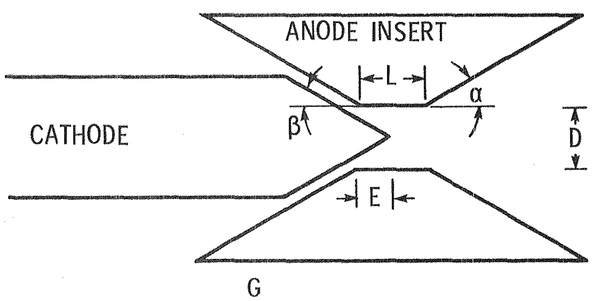


Figure 3. - Cathode/anode dimensions.

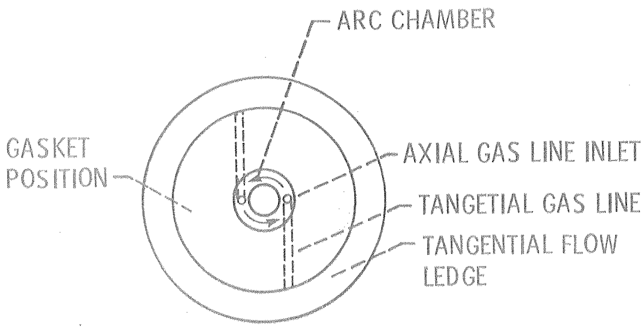


Figure 4. - Boron nitride insulator with gas passages.

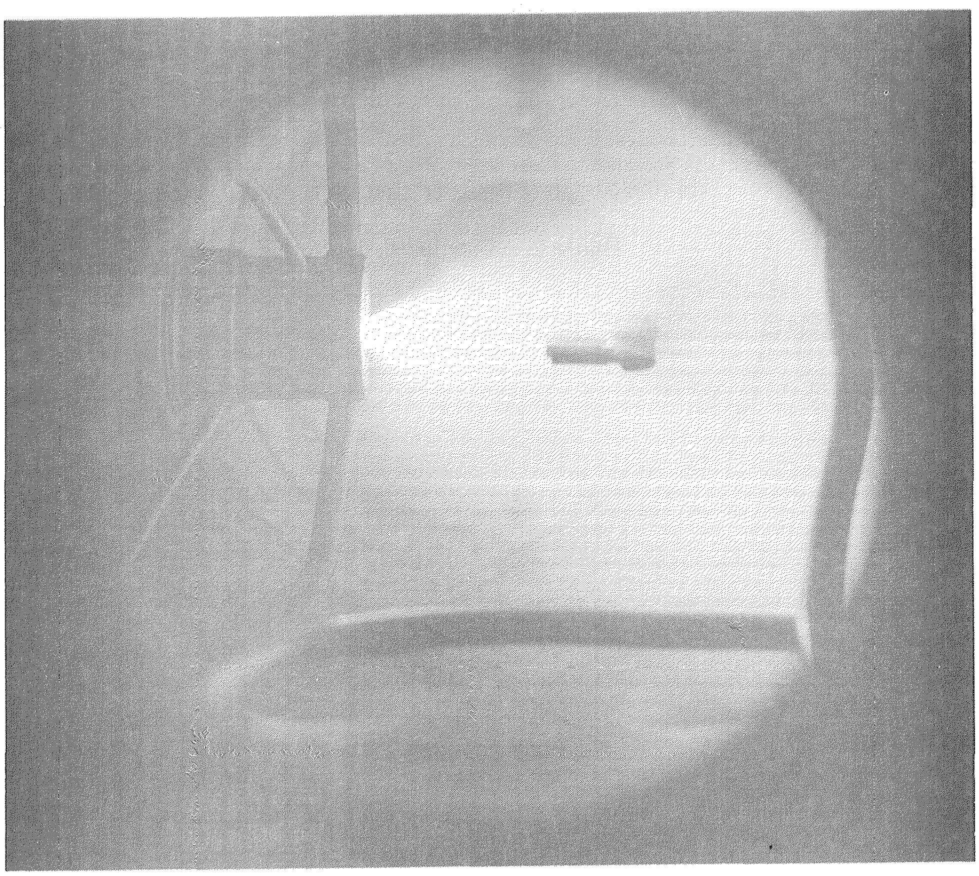

(a) Arcjet simulator operating with argon.

Figure 5. - Photographs of arcjet simulator in operation.

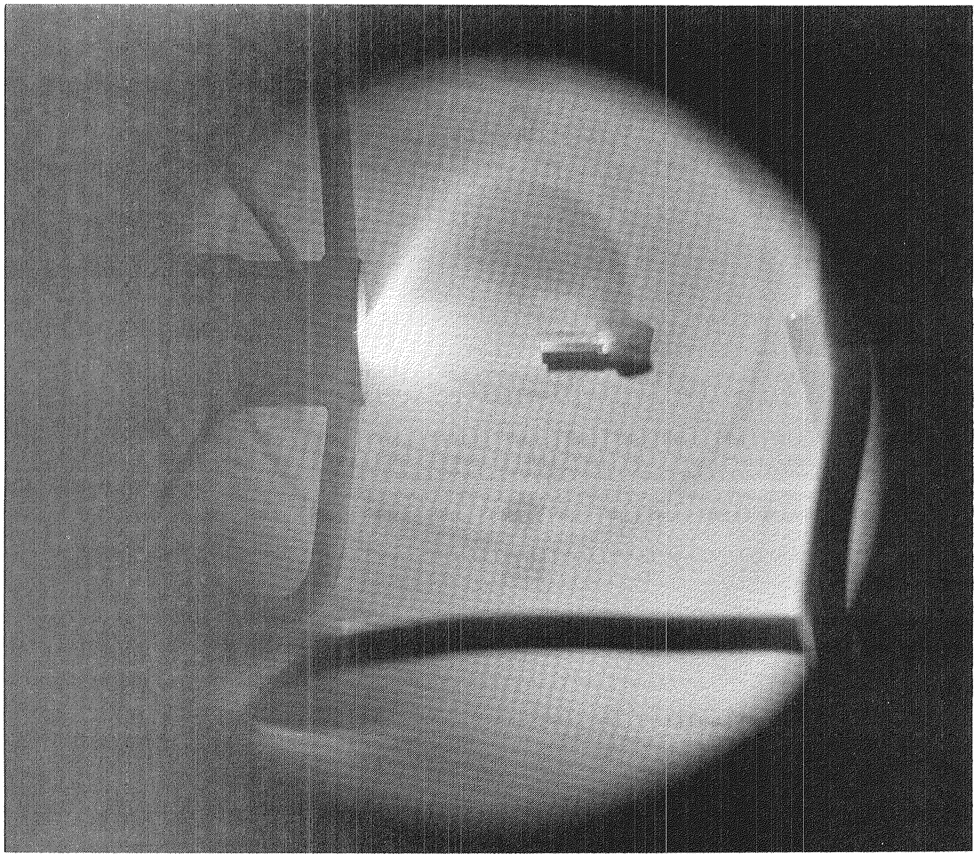

(b) Arcjet simulator operating with nitrogen.

Figure 5. - Concluded.

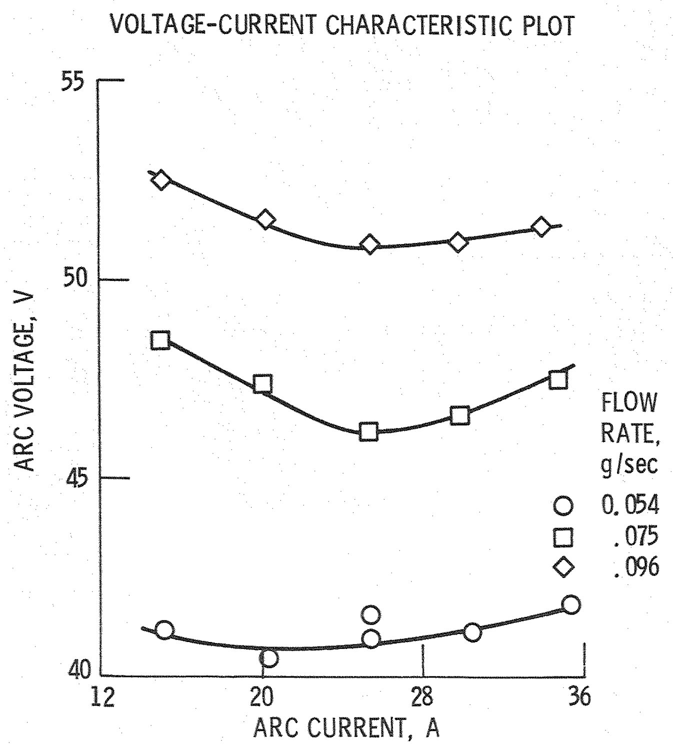


(a) Voltage-current characteristic plot; test number 78.

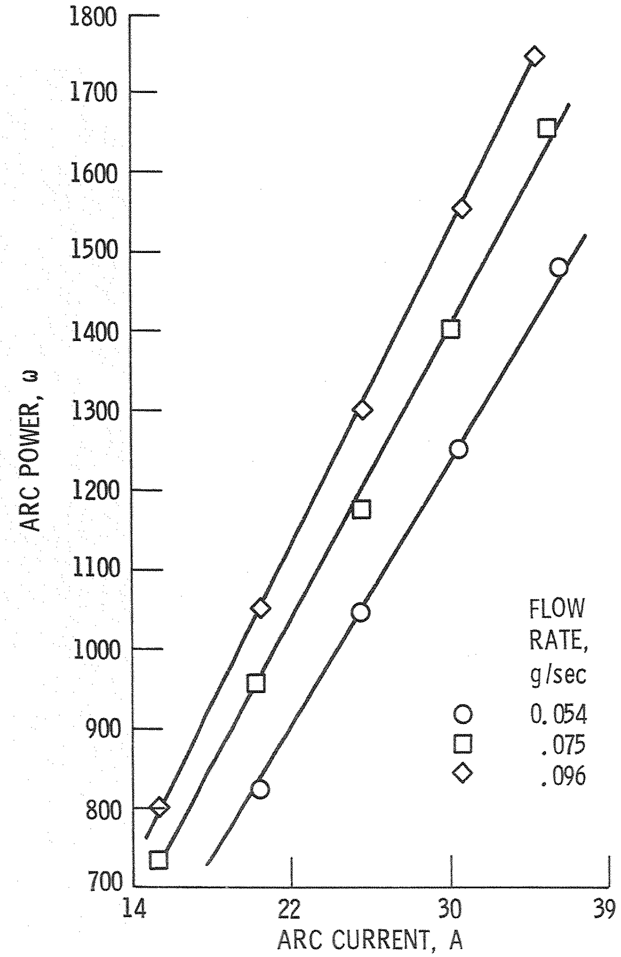


(b) Arc power versus current; test number 78.

Figure 6. - Typical results - power input characteristics.

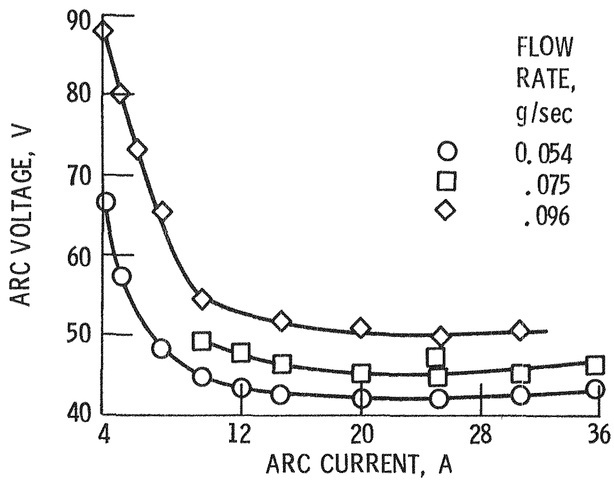


Figure 7. - Voltage/current characteristics; test number 85.

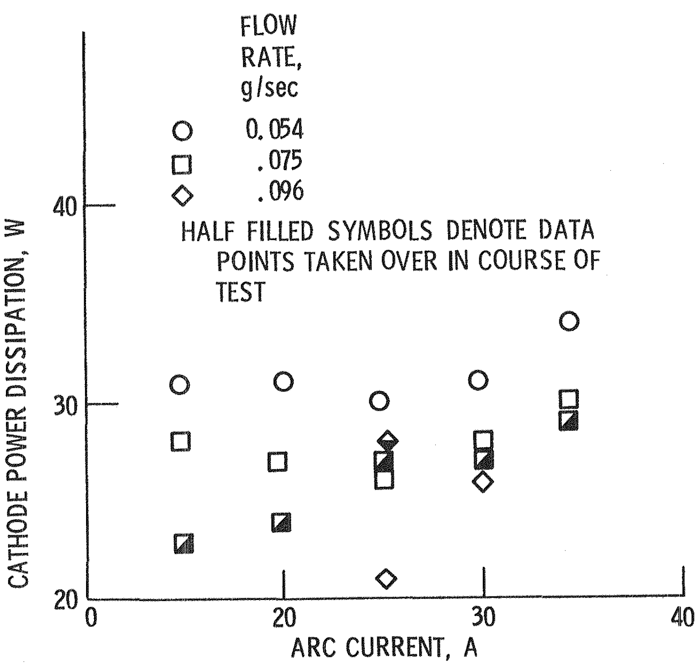


Figure 8. - Cathode power loss versus current; test number 84.

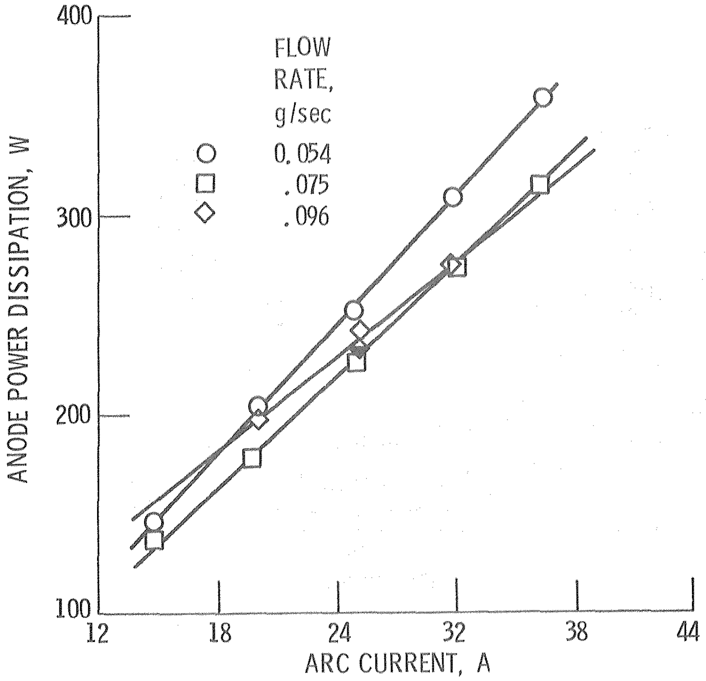


Figure 9. - Anode power loss versus current.

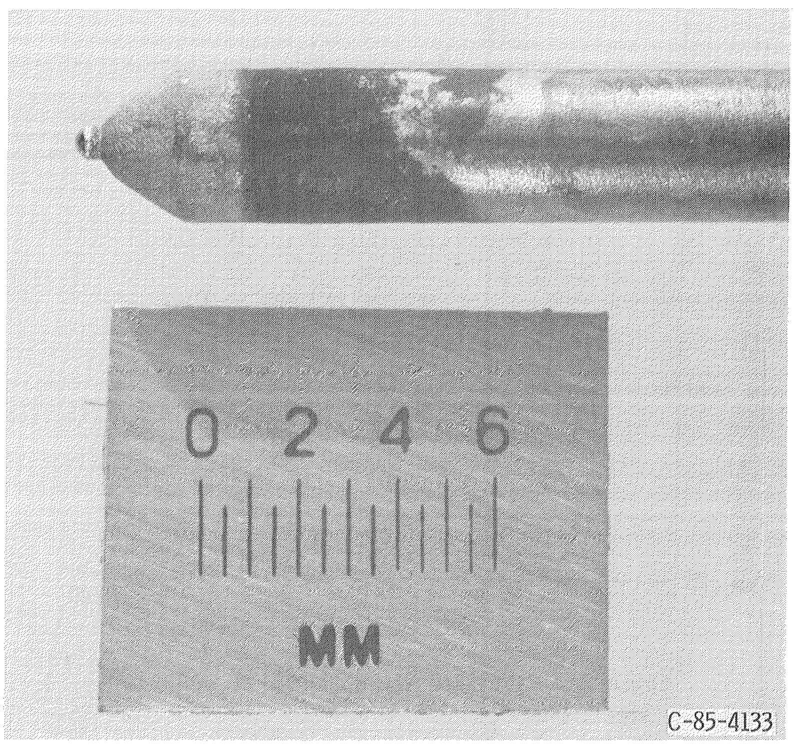


Figure 10. - Photograph of cathode; test #76.

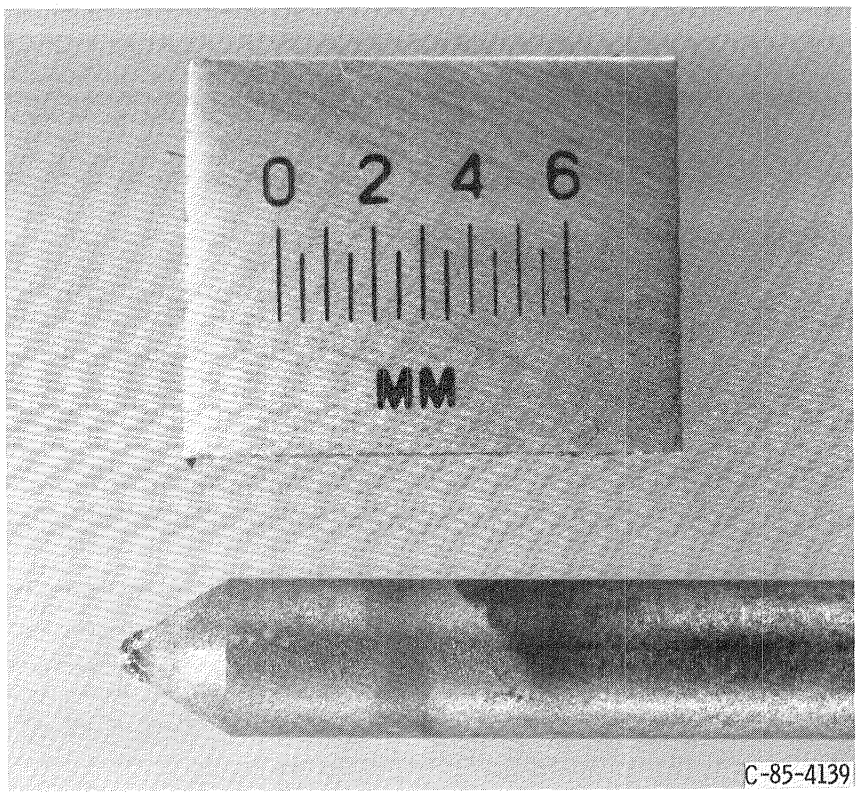


Figure 11. - Photograph of cathode; test #80.

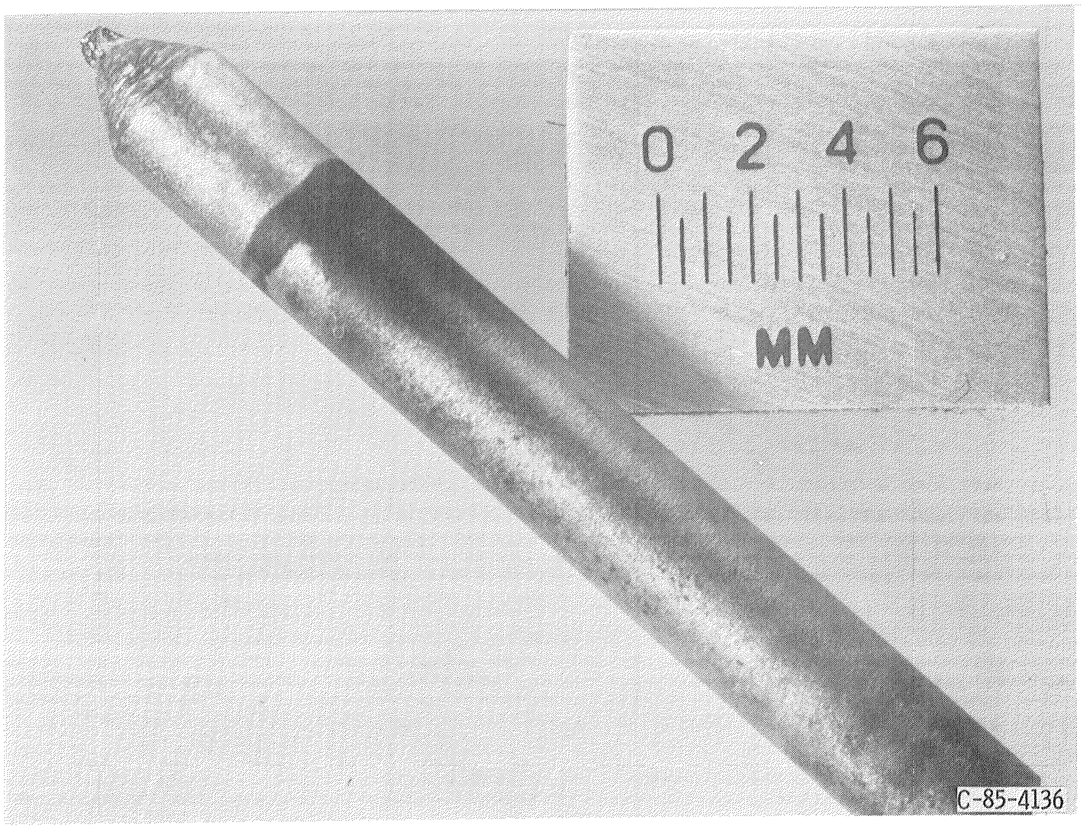


Figure 12. - Photograph of cathode ; test #78.

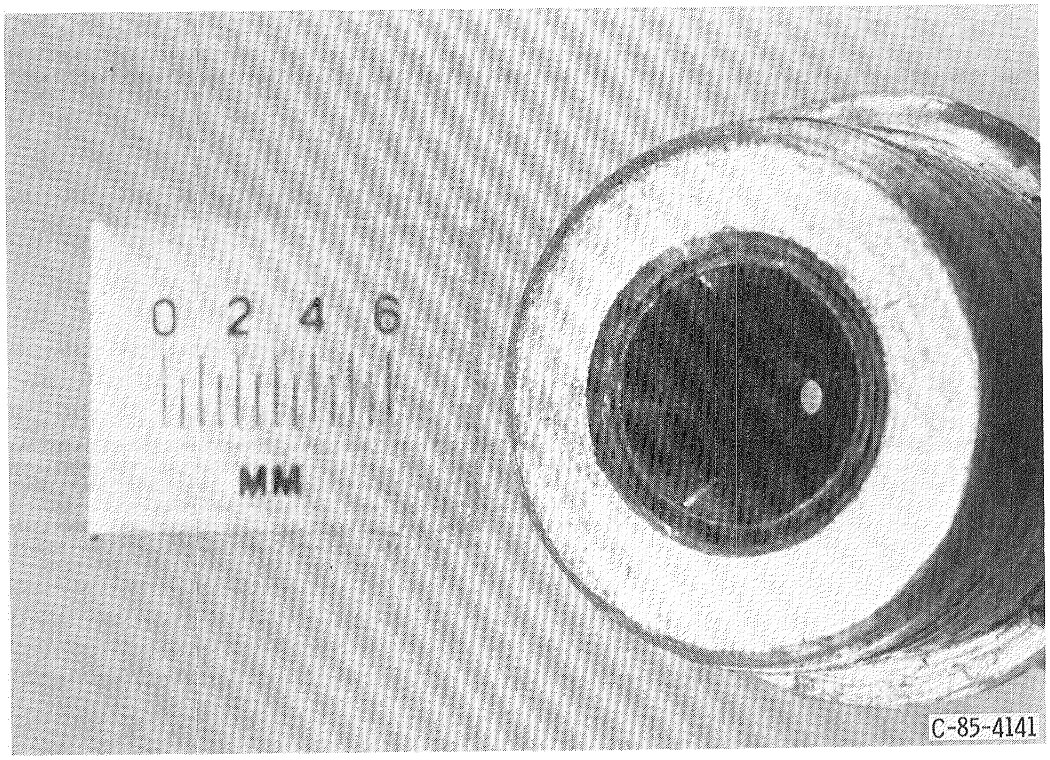


Figure 13. - Anode section, nozzle side and constrictor; test #84.

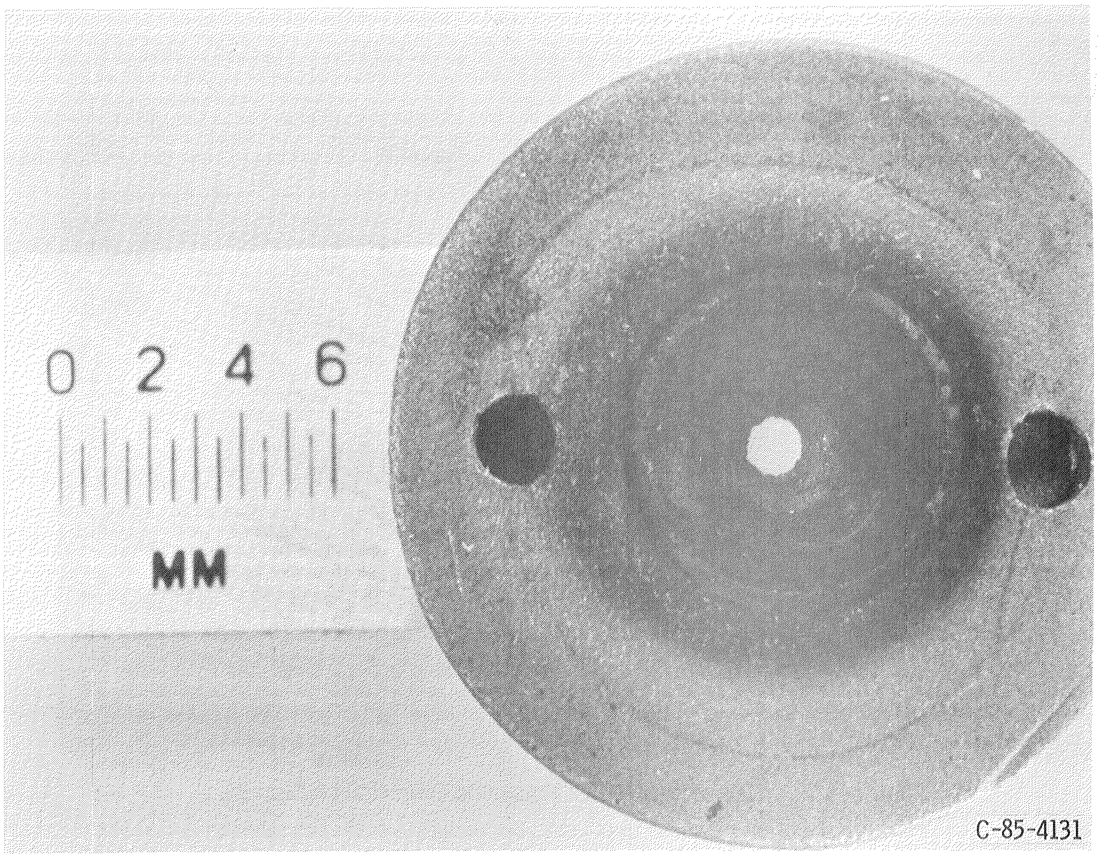


(a) Anode section, arc chamber side; test #76.

Figure 14. - Photograph of anode.

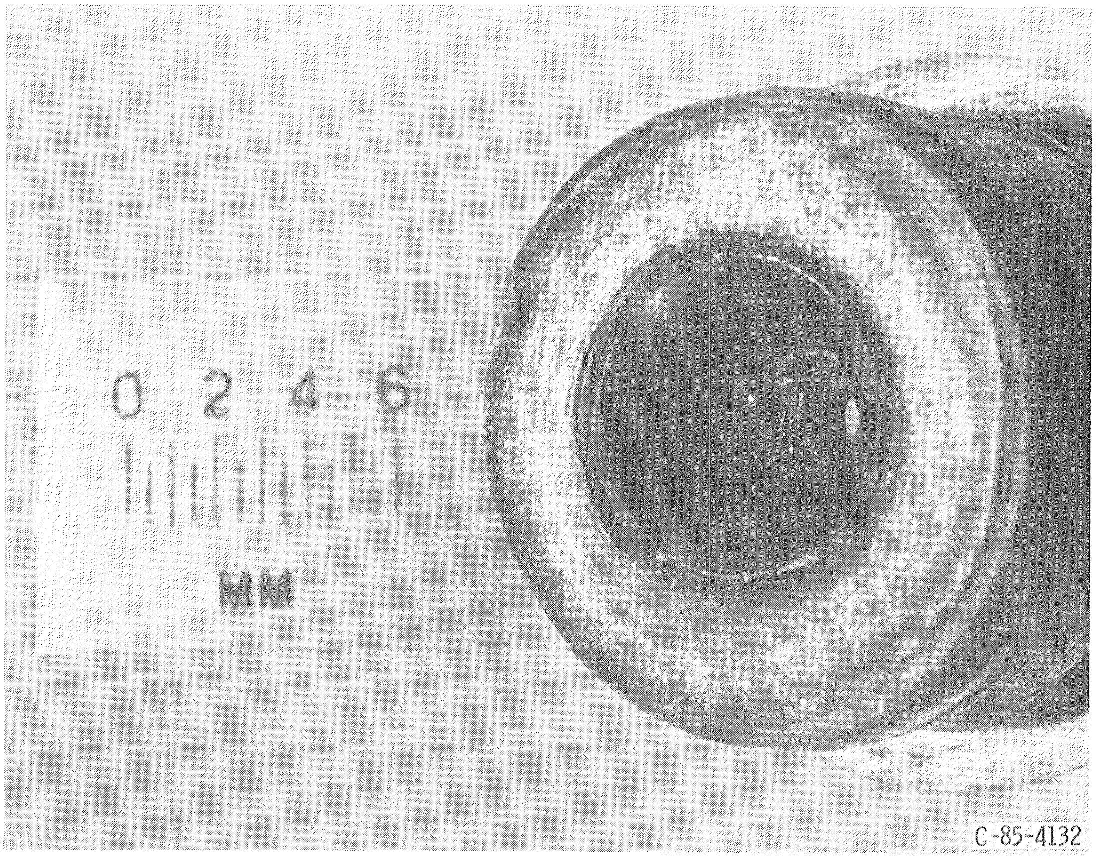


(b) Anode section, nozzle side and constrictor ; test #76.

Figure 14. - Concluded.

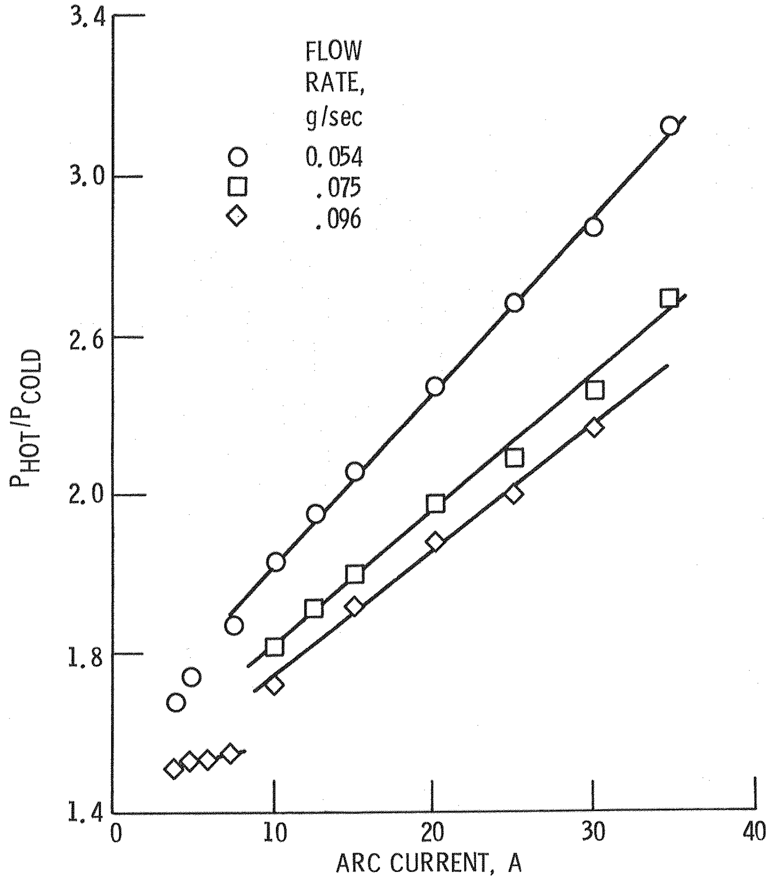


Figure 15. - Hot to cold pressure ratio; test number 85.

| 1. Report No. NASA TM-87123 AIAA-85-2017 | 2. Government Accession No. | 3. Recipient's Catalog No. |
|---|---|---|

| 4. Title and Subtitle | 5. Report Date |
|---|---|
| An Experimental Study of Energy Loss Mechanisms and Efficiency Considerations in the Low Power dc Arcjet | 6. Performing Organization Code 506-55-22 |
| 7. Author(s) Francis M. Curran | 8. Performing Organization Report No. E-2733 |
| | 10. Work Unit No. |
| 9. Performing Organization Name and Address National Aeronautics and Space Administration Lewis Research Center Cleveland, Ohio 44135 | 11. Contract or Grant No. |
| | 13. Type of Report and Period Covered Technical Memorandum |
| 12. Sponsoring Agency Name and Address National Aeronautics and Space Administration Washington, D.C. 20546 | 14. Sponsoring Agency Code |

15. Supplementary Notes

Prepared for the Eighteenth International Electric Propulsion Conference cosponsored by the AIAA, JSASS, and DGLR, Alexandria, Virginia, September 30 - October 2, 1985.

16. Abstract

The potential utility of the low power dc arcjet in the field of auxiliary propulsion has motivated research activities at NASA Lewis Research Center and elsewhere. Early work in the field indicated that improvements in the areas of stability, energy efficiency, reliability, and electrode erosion would be necessary to obtain a useful device. Experiments with a water-cooled arcjet simulator were performed to investigate both the energy loss mechanisms at the electrodes and the stability of different conventional arcjet configurations in the presence of a vortex flow field. Although a full parametric study has not been completed, preliminary results show that in certain configurations only 25 to 30 percent of the input energy is lost to the electrodes. Results also show that vortex stabilization is not difficult to obtain in many cases at the flow rates used (0.054 to 0.096 g/sec $N_2$) and that a careful starting procedure is effective in minimizing electrode damage.

| 17. Key Words (Suggested by Author(s)) | 18. Distribution Statement |
|---|---|
| Arcjet; Low power arcjet; Efficiency | Unclassified - unlimited STAR Category 20 |

| 19. Security Classif. (of this report) | 20. Security Classif. (of this page) | 21. No. of pages | 22. Price* |
|---|---|---|---|
| Unclassified | Unclassified | | |

*For sale by the National Technical Information Service, Springfield, Virginia 22161

**End of Document**